JOURNAL OF SPACECRAFT AND ROCKETS
Vol. 42, No. 3, May–June 2005

Solar Arrays for Direct-Drive Electric Propulsion: Arcing at High Voltages

Todd A. Schneider*
NASA Marshall Space Flight Center, Huntsville, Alabama 35812
I. G. Mikellides† and G. A. Jongeward‡
Science Applications International Corporation, San Diego, California 92121
and
T. Peterson,§ T. W. Kerslake,¶ D. Snyder,** and D. Ferguson††
NASA John H. Glenn Research Center at Lewis Field, Cleveland, Ohio 44135

The results from an experimental investigation to assess arcing during operation of high-voltage solar arrays in a plasma environment are presented. The experiments were part of an effort to develop systems that would allow safe operation of Hall-effect thruster(s) in direct-drive mode. Arc discharges are generated when the array is biased negative with respect to the plasma. If sustained for long periods of time between adjacent solar cells, arcs can severely damage a solar array, thus significantly shortening its lifetime. Most often sustained arcs are triggered by plasma produced during short-duration discharge arcs (∼20 ms). These "trigger" arcs are sparked between the semiconducting cell and the covering dielectric. Both trigger and sustained (>1-ms) arcs have been captured during the tests. Current and voltage waveforms associated with the different arc events are presented. The test results have defined operational limits (thresholds) for the various array concepts studied that minimize the likelihood of damage from sustained arcs. Experimental trends regarding the effect of the solar-array substrate on arc duration are also presented.

Introduction

A GUIDING precept of spacecraft design is to seek out savings in system mass as well as power system efficiency. Consequently, work is being conducted in the aerospace industry to create high-voltage low-current solar-array systems, which allow the use of smaller current-carrying conductors in the power generation and distribution systems. The usefulness of high-voltage solar arrays has been further refined for the case of spacecraft that employ Hall-effect thrusters (HET).[1,2] In this case, considerable savings could be realized by driving the thruster directly from a high-voltage array.[3] Such a system would significantly reduce the weight and complexity of the power processing unit, which is commonly used to step up the array voltage.

Previous work suggested the operation of a Hall-effect thruster in direct-drive mode is feasible.[4] However, no detailed tests were performed to assess life-limiting issues, such as arcing, associated with prolonged operation of such a high-voltage system in a Hall-effect-thruster plasma environment. The present work is part of a larger effort that aims (in part) to identify requirements for the safe operation of a direct-drive Hall-effect thruster (D2HET) system. A more specific objective of the D2HET program is to identify solar-array technologies that are capable of operating at high voltages in the charge-exchange plasma environment induced by the HET. Naturally, technologies developed for this particular application will also be relevant to other spacecraft that operate with high-voltage solar arrays in a dense plasma environment (e.g., low-earth-orbit ionosphere). As NASA looks to high-power electric propulsion, lessons learned from the D2HET program promise to elucidate many of the serious interaction issues associated with high-voltage spacecraft systems in a dense plasma environment.

Among others, the solar array must operate under two major requirements: 1) minimal electron current collection, also known as parasitic or leakage currents, by the solar array and 2) no prolonged arcing across adjacent cells. Parasitic currents can degrade the performance of the solar array and can become a significant design obstacle if the collected electron current is a substantial fraction (more than a few percent) of the array operating current. Sustained arcing can lead to permanent electrical shorts and has been found to occur only when parts of the array are at negative electric potentials and can therefore attract ions. (No arc events were observed when the array was biased positive.)

Our current understanding of the arc process is based on earlier experiments conducted by Vaughn et al. in support of the International Space Station.[5] Arcs were initiated on biased anodized aluminum in a background plasma. The experiments confirmed that a trigger arc releases a plasma that expands from the arc site and covers the nearby surfaces with a low impedance plasma. If there is positive charge on the surfaces, the plasma can conduct electrons from the arc site to the surface, thereby discharging the effective capacitance of the surface. This configuration occurs when a chassis is negative with respect to a background plasma. For the D2HET system we expect this to occur in low Earth orbit when the HET is off and the arrays are generating 300 V, causing the system to float negative. In geosynchronous orbit or higher orbits where magnetospheric environments can induce inverted chassis voltages, then ion collection will also occur.

Ground tests have been performed under conditions of both electron and ion collection. Results from the electron collection tests,

Presented as Paper 2003-5017 at the AIAA/ASME/SAE/ASEE 39th Joint Propulsion Conference, Huntsville, AL, 20–23 July 2003; received 6 October 2003; revision received 7 April 2004; accepted for publication 15 April 2004.

*Physicist, ED31, Space Environmental Effects Group. Member AIAA.
†Scientist; currently Scientist, Mail Stop 125-09, Advanced Propulsion Technology Group, Jet Propulsion Laboratory, California Institute of Technology, Pasadena, CA 91109. Member AIAA.
‡Division Manager, Mail Stop X1, Defense Technology Group, 10260 Campus Point Drive.
§Program Manager, 500-103, Power and Propulsion Office, 21000 Brookpark Road.
¶Aerospace Engineer, 500-103, Power and Propulsion Office, 21000 Brookpark Road.
**Electrical Engineer, 302-1, Photovoltaics and Space Environments Branch, 21000 Brookpark Road. Member AIAA.
††Group Leader for Space Environments, 302-1, Photovoltaics and Space Environments Branch, 21000 Brookpark Road. Senior Member AIAA.

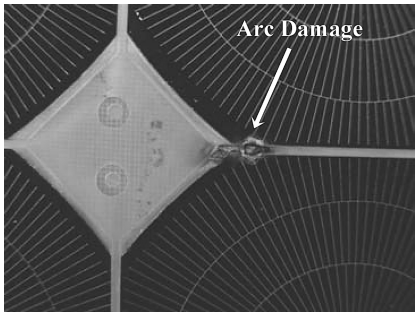

Fig. 1 Arc damage on a section of coupon 1.

as well as from modeling and simulation efforts, are presented by Mikellides et al.[6] In this paper, we focus on results from arcing tests using sample coupons that are based on two main solar-array technologies. During the tests, the coupons were biased to hundreds of volts negative with respect to the plasma.

Arcing on solar arrays has been shown to result in significant damage.[7] Arc events can damage not only individual photovoltaic cells, but also entire strings of cells if the discharge leads to an electrical short between strings.[8] Such arcs typically occur at large negative voltage bias (<-100 V). Past work has exposed two main types of arcs: 1) short-duration electrical discharges, termed in this paper trigger arcs, and 2) long-duration arc discharges termed in this paper sustained arcs.[9–12] A typical trigger arc current signal peaks at high values (>20 amps) but lasts for only a short time (<50 μs). Trigger arcs are benign and most often do not cause permanent damage. They can, however, lead to prolonged arcs, which as alluded to earlier, can cause severe damage depending on the conditions under which the discharge is sustained. Sustained arcs are characterized by relatively low currents (<10 A) and very long duration (from hundreds of microseconds to tens of seconds). Sustained arcs most commonly occur when a potential difference exists between cells, usually two cells adjacent to each other along a string. It has been suggested that the dense plasma created by a trigger arc on one cell bridges the gap between adjacent cells by providing a conductive path between the differentially biased cells, which results in current flow between the cells.[13] Figure 1 shows a damaged section of a solar-array coupon that occurred during testing reported in this effort. The damage was caused by an arc across adjacent cells that lasted for 0.5 s. Additional examples of damage that have resulted from sustained arc events are available in the literature.[11,14]

The tests described in this paper have focused on determining the conditions under which trigger arcs and sustained arcs occurred on solar-array sample coupons that were negatively biased in a plasma environment. Descriptions of the different solar-array sample configurations are provided, as well as examples of current and voltage waveforms. In addition, the results are analyzed to identify trends that can help guide future theoretical work and mitigation techniques.

Experiment Description

A major goal in the development of a direct-drive electric propulsion system is to identify solar-array technologies that can be operated safely in a HET plasma environment. Three technologies have been tested. The first technology is based on the design used for the International Space Station (ISS). ISS solar arrays have been designed to operate at relatively high voltage (160 V) and have demonstrated continuous operation in space for years. An attractive feature of the ISS design is that interconnects are completely covered by a dielectric film (Kapton). However, the cell (semiconductor) edges are not insulated and are therefore exposed to the plasma. The ISS array sample, which we will refer to as coupon 1 in this paper, is shown in Fig. 2. The solar array coupon consists of three rows of cells with five cells in each row. Each individual cell has the shape of a square with all four corners cut at approximately 45 deg. The primary dimensions of each cell are 0.08×0.08 m. Each silicon solar cell is single junction.

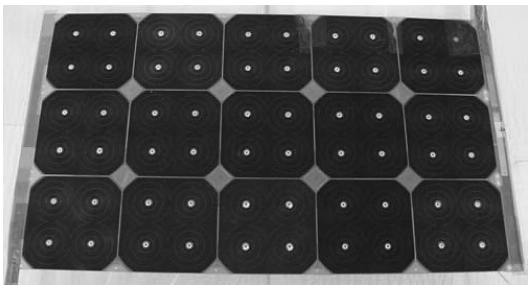

Fig. 2 Top view of coupon 1.

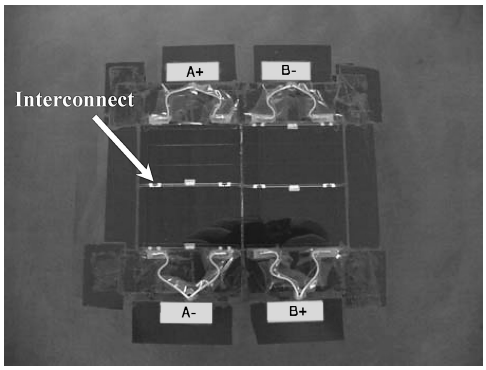

Fig. 3 Top view of coupon 2.

In contrast to coupon 1, the second technology tested employs exposed interconnects as shown in Fig. 3. The cells on the coupon (termed coupon 2 in this paper) are mounted on top of a thin Kapton film (a few thousandths of an inch). The film in turn rests on top of a rigid structure formed from graphite sheets with an aluminum honeycomb structure in the middle, as shown in Fig. 4a. The solar cells of coupon 2 are representative of the newer, more efficient advanced-triple-junction technologies that utilize indium/gallium/arsenide/germanium semiconducting materials. Each cell is rectangular in shape and has the dimensions 0.038×0.064 m. A variant of this version (termed coupon 3 in this paper) that can offer significant increase in solar-array output is the technology with concentrators, as shown in Fig. 4b. The concentrator (the triangular shape located between the two photovoltaic modules in Fig. 4) is made of thin metallized dielectric film. The test results presented here focus on the base technologies, namely, coupons 1 and 2; however, arc threshold voltages are also presented for coupon 3.

Individual "mock cells," not part of any of the designs just described, have also been tested in various arrangements. The cells are geometrically similar to the ISS cells. However, each cell is made of copper instead of the semiconducting material used in the ISS coupon. The main goal behind the mock cell tests was to assess (with relative ease) the effects of different geometrical arrangements of the cells on arcing.

Regardless of the particular test coupon used, each sample shared some common characteristics as illustrated in Fig. 5. First, all samples shared the same Kapton film on top of their substrates (except for the last case to be described later). Second, there was no encapsulation of the solar cells, that is, the semiconductor sides were exposed to the plasma, and, third, silica-based dielectric material (coverglass) was layered on top of all solar cells as shown in Fig. 5. In coupon 1 and the test (or mock) cells the coverglass sheet overhung by a few mils (1 mil = 1/1000 in.) beyond the cell material. There was no coverglass overhang in coupons 2 or 3.

The vacuum chamber employed for the experiments is cylindrical in shape with a 1.22 m inside diameter and a useable length of 1.73 m. The chamber is a diffusion pumped chamber with liquid-nitrogen traps above each pump and typical base pressure of 5×10^{-7} torr. Mounted on one end of the chamber is a hollow cathode plasma source that operated with argon gas. The "keeper" electrode on the source was grounded to reduce the electric field interaction

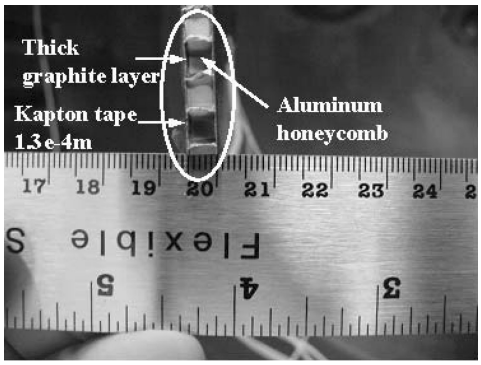

a)

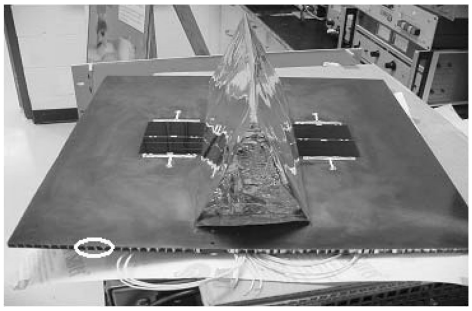

b)

Fig. 4 Side view of coupon 3 showing concentrator.

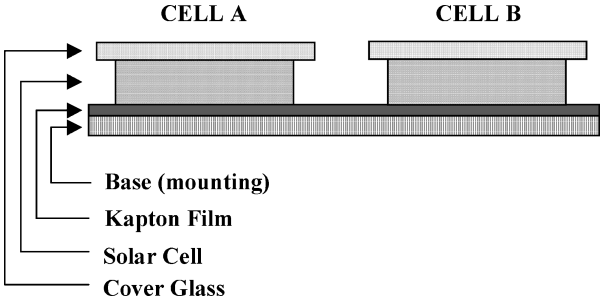

Fig. 5 Side view drawing of a typical solar-array coupon.

between the biased samples and the emitter in the source. At a typical operating pressure in the chamber of 8×10^{-5} torr, the plasma source generated a plasma with particle density of $5–10 \times 10^{6}$ cm^{-3}, electron temperature 0.5–1 eV, and plasma potential of about −20 V. All plasma parameters were measured with a gold-coated aluminum spherical Langmuir probe, which was coplanar with the solar-array samples. Figure 6 is a representative drawing of the chamber and equipment used for the experiments.

Two basic electric circuits were produced for biasing the coupons and diagnosing their interactions with the plasma. The first circuit was configured to generate and measure trigger arcs; the second was designed for sustained arcs. Figure 7 depicts a simplified picture of the trigger arc circuit. A key component to this circuit is the capacitor. Because of obvious vacuum chamber size constraints, it was not possible to test full-size solar arrays, which have a significant self-capacitance. Therefore, to appropriately simulate the capacitance of a full array, while only using a small sample, an external capacitance was added to the circuit. A value of 1 microfarad was chosen based on the two sample missions referenced in the D2HET program, namely, the Deep Space-1 (DS-1) and EXPRESS missions.[15] The capacitor was connected to the charging power supply via a large resistor (500,000 ohms). This resistor was placed to decouple the power supply from the arc event. In this arrangement, once an arc occurred, the power supply only contributed a very small current to the arc. Energy to the arc was therefore fed strictly from the capacitor (and the applied voltage), which closely simulates how such an event would evolve on orbit.

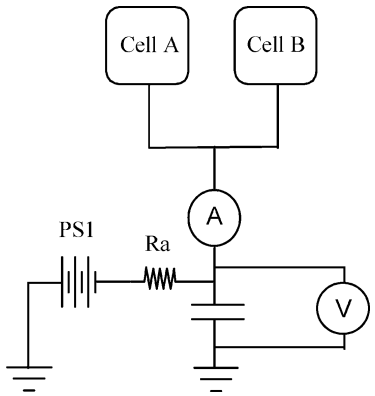

Fig. 7 Schematic drawing of the basic components in the trigger-arc circuit.

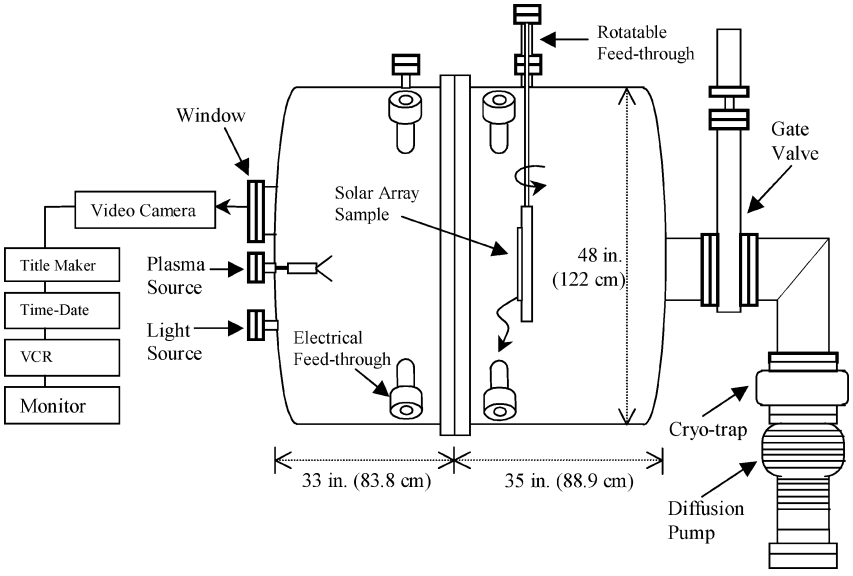

Fig. 6 Drawing of the plasma test chamber.

Figure 8 illustrates a simplified version of the sustained arc circuit. The main distinction between the two circuits (Figs. 7 and 8) is the addition of a second power supply in the second circuit (Fig. 8). This power supply was a dc power supply (Sorensen DCR 300-6B). This second power supply is added to provide a differential voltage between adjacent cells. The voltage drop emulates the potential difference that can exist in a flight solar array between adjacent cells located along a string.

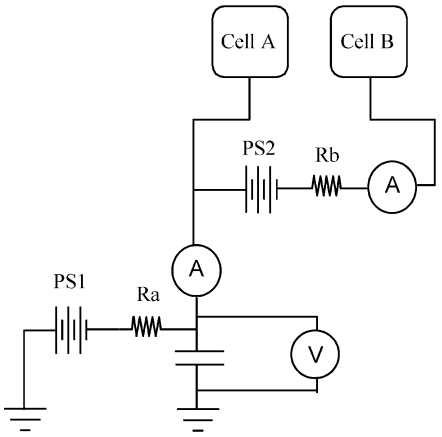

Fig. 8 Schematic drawing of the basic components in the sustained-arc circuit.

The data-acquisition methodology remained fairly unchanged throughout all of the tests. A personal computer equipped with a data-acquisition card and an IEEE-488 card was operated to facilitate the tests. A program was written to control the data-acquisition system. The program set the power supply voltages, controlled all of the switches in the circuit, detected the occurrence of an arc, shut off the power supplies, and transferred the data from the digital storage oscilloscopes. Figure 9 is a more detailed representation of the sustained arc circuit and pertinent equipment employed during the tests.

Test Results

The first tests conducted on each of the array coupons aimed to record trigger arcs and identify a regime of operation under which the arc rate was significantly reduced. For these tests, all of the cells on a sample were connected together and biased at the same voltage using the trigger arc circuit just described. An example of a trigger-arc voltage and current waveform is shown in Figs. 10 and 11 from coupons 1 and 2, respectively. Although the individual waveforms are of interest, the focus of the trigger-arc testing was to determine the trigger-arc threshold voltage for each array sample. "Threshold" in the present investigation is defined loosely as the bias voltage below which the coupon in question did not arc for more than one hour. It is therefore recognized that the trigger-arc threshold results presented herein provide only a direction for significantly reducing the arc rate; not to eliminate completely the possibility of arcing under real space conditions. To determine the trigger-arc threshold, the procedure shown in Fig. 12 was followed. The results of the threshold testing for the different array samples are tabulated in Tables 1–3.

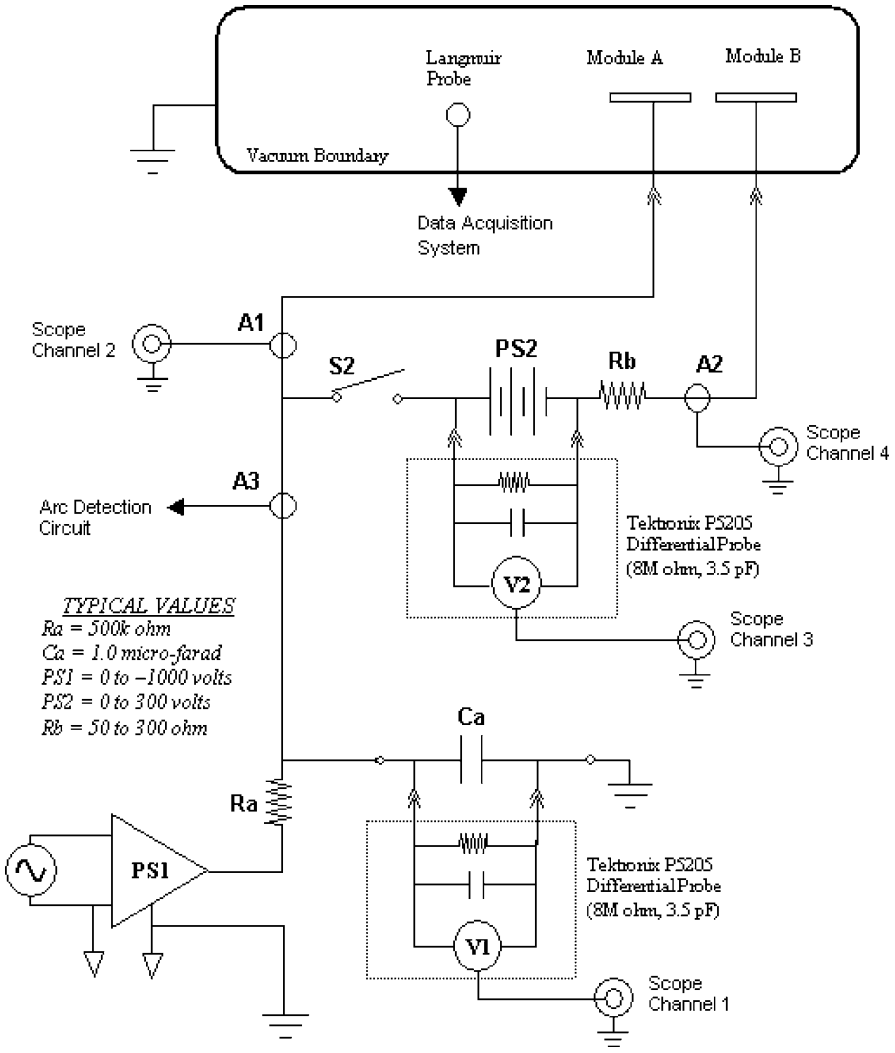

Fig. 9 Detailed schematic of the sustained-arc circuit.

To simulate conditions under which sustained arcing could occur, a differential voltage was applied between cells. The array wiring was modified so that two cells (or strings) could be electrically separated, as shown in Fig. 8. To generate the short discharges that typically trigger the prolonged discharges between cells, the capacitor was charged to a voltage that is well above the trigger-arc threshold voltage (typically less than −700 to −500 V). Initially, the differential power supply was set to a low voltage and then

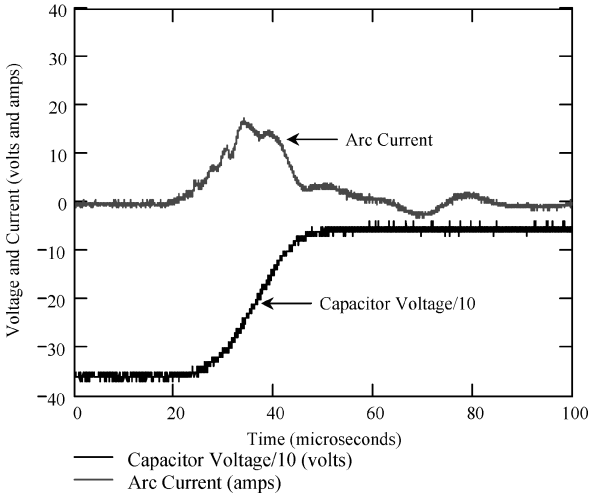

Fig. 10 Typical trigger-arc waveforms associated with coupon 1.

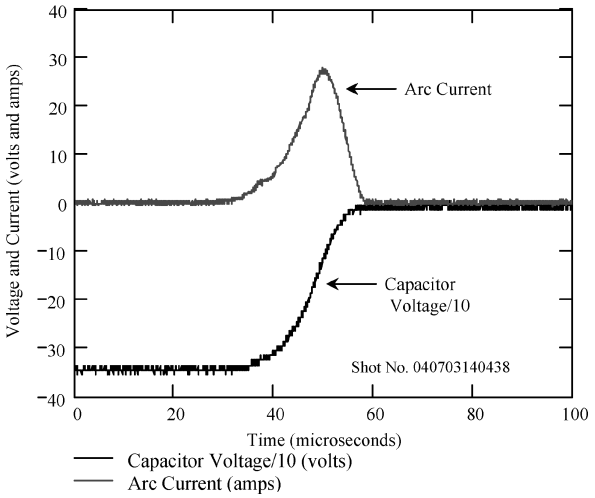

Fig. 11 Typical trigger-arc waveforms associated with coupon 2.

Table 1 Trigger-arc threshold test results for coupon 1

Applied voltage, V	Time elapsed before arc, min
Day 1 test	
−500	0.159
−450	1.629
−400	24.985
−350	60
−360	60.001
−370	49.416
Day 2 test	
−400	9.981
−350	60.001
−360	60.001
−370	10.979
−400	27.474
−350	60.001
−360	34.361

Table 2 Trigger-arc threshold test results for coupon 2

Applied voltage, V	Time elapsed before arc, min
Day 1 test	
−400	1.059
−350	0.507
−300	19.618
−250	28.504
−200	60.001
−210	24.885
Day 2 test	
−250	12.636
−200	60.001
−210	54.448

Table 3 Trigger-arc threshold test results for coupon 3: day-1 test

Applied voltage, V	Time elapsed before arc, min
−400	0.013
−350	0.024
−300	0.059
−250	0.266
−200	60.001
−210	0.874

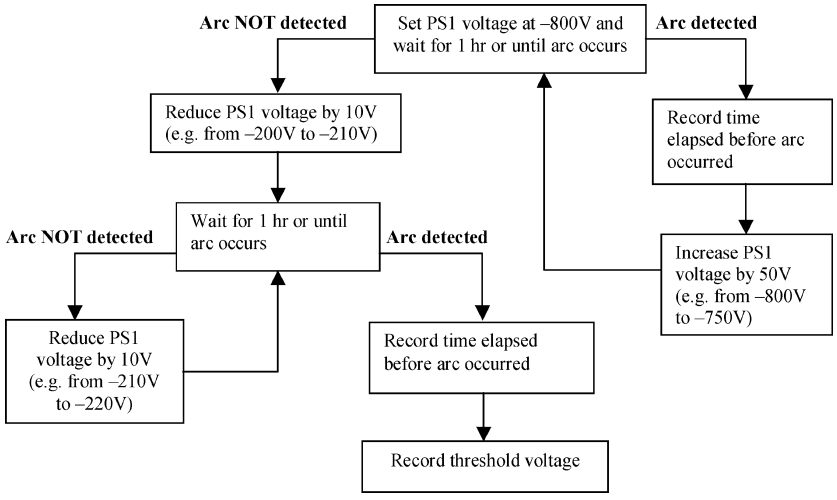

Fig. 12 Procedure used to determine the arc threshold voltage.

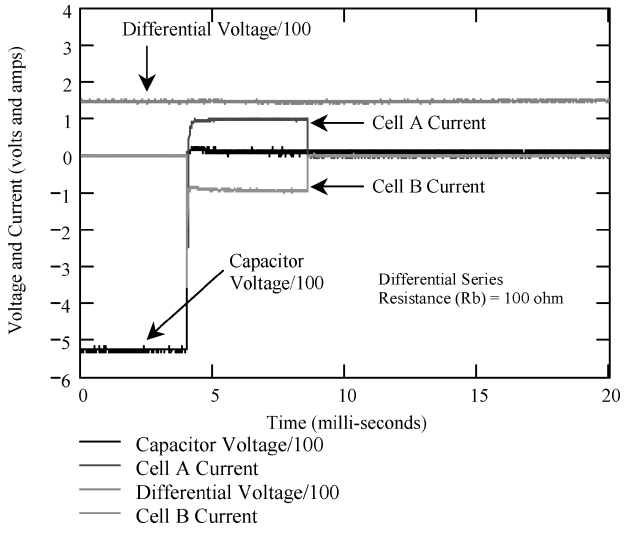

Fig. 13 Typical sustained-arc waveforms associated with coupon 1.

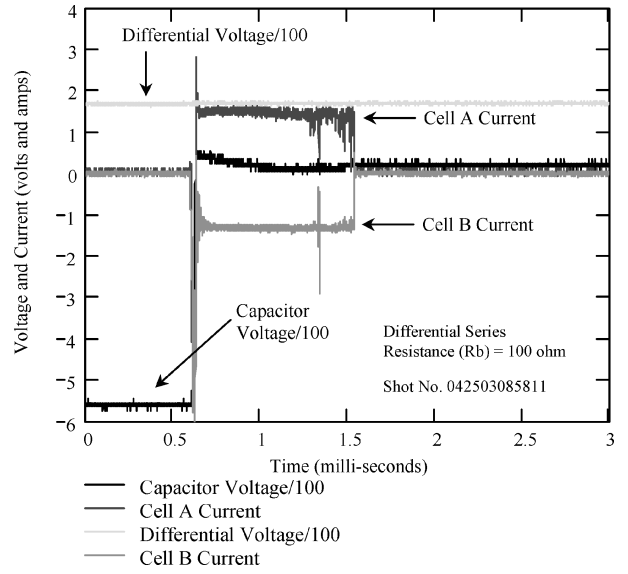

Fig. 14 Typical sustained-arc waveforms associated with coupon 2.

increased until a sustained arc occurred. It is noted that a resistor R_b was placed in series with the differential power supply. This resistor was used to control the maximum current available to the arc. The resistance was changed based on the voltage level of the differential power supply. In most cases the circuit was limited to less than 3 amps of current flow between cells. Typical current and voltage waveforms associated with sustained arcs occurring on coupons 1 and 2 are shown in Figs. 13 and 14, respectively. (No sustained arcs were generated on coupon 3. Presumably this is because of the large separation between cells necessary to accommodate the triangular reflector.) In both Figs. 13 and 14, the differential voltage stays constant even during the arc event. This is because the measurement of the voltage was made across the PS2 power supply and not across the cell gap (see the schematic shown in Fig. 9). However, as is described next, the arc voltage across the gap was determined based on the measured arc current and the known resistance in the circuit.

By limiting the current and voltage in the differential circuit, it was possible to examine sustained arc thresholds as a function of voltage, current, and power (voltage × current). Specifically, to determine the voltage drop V_p across, and the power available P_{arc}, in each recorded arc the sustained current I_s was averaged from the pulse signal (e.g., Figs. 13 and 14), between the time that sustainment began (i.e., upon end of the trigger arc) until the arc was abruptly quenched. This steady-state value was then used to estimate V_p and

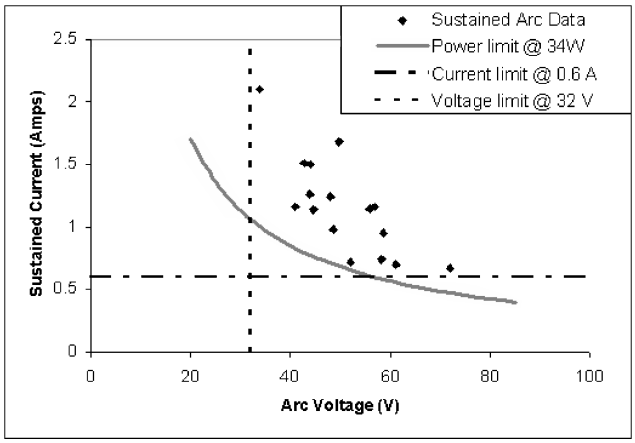

Fig. 15 Results of sustained-arc testing on coupon 1. Limits on the generation of a sustained arc are shown.

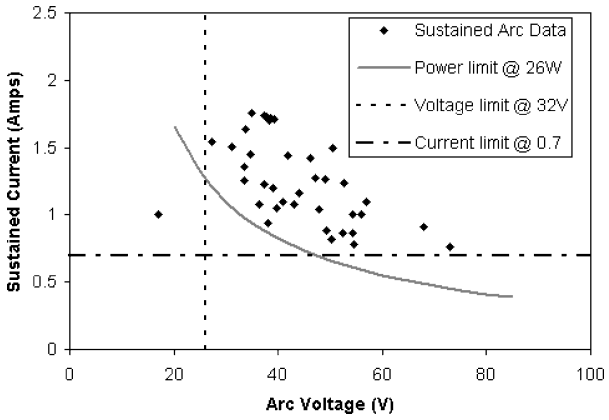

Fig. 16 Results of sustained-arc testing on coupon 2. Limits on the generation of a sustained arc are shown.

P_{arc} as follows:

$$V_p = V_{\text{PS2}} - I_s R_b, \qquad P_{\text{arc}} = I_s V_p \tag{1}$$

where V_{PS2} is the voltage applied by power supply PS2 and R_b is the value of the current-limiting resistor (Fig. 9). Figures 15 and 16 summarize the results of the sustained-arc tests for coupons 1 and 2, respectively.

It is possible that material from solar-cell components can play a significant role in the sustainment of the discharge across adjacent cells. For example, it is possible that heating of the substrate material leads to the release of neutral particles from the surface, through evaporation or even ablation. Depending on the rate with which these neutrals are released into the discharge, the local ionization rate, and the rate with which electrons are released from the conducting materials, the duration of the arc can change significantly. The role of the substrate material in particular is not well understood. In view of the relative ease with which different substrate materials can be substituted, a simple test was conducted by using the mock cells. A mock cell setup was constructed that had two cells mounted "flat" against the Kapton substrate, similar to the cell arrangement of coupon 1. In addition, two mock cells were elevated 5 cm above the Kapton substrate to emulate a cell pair without a substrate. A side view of this solar-array sample is shown in Fig. 17. Sustained-arc tests were conducted on the samples, and the arc duration between the flat cells and the elevated cells is compared in Fig. 18. In this figure it is evident that the elevated cells sustained arcs for a longer period of time than the flat cells. In some cases the elevated cells (no substrate) maintained an arc for a time period that was more than an order of magnitude longer than the flat cells. The results provide an indication that it might be possible to minimize the arc duration by choosing a substrate material that will "quench" the arc.

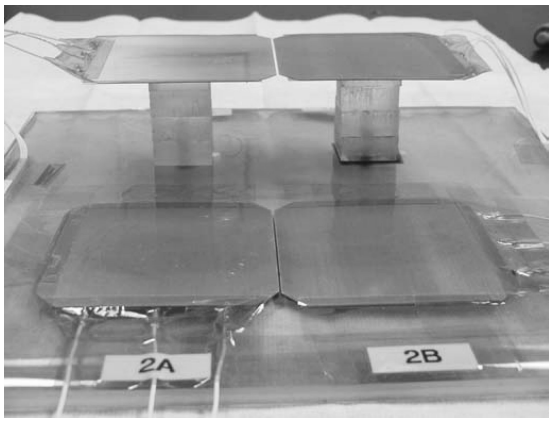

Fig. 17 Picture of the mock array coupon.

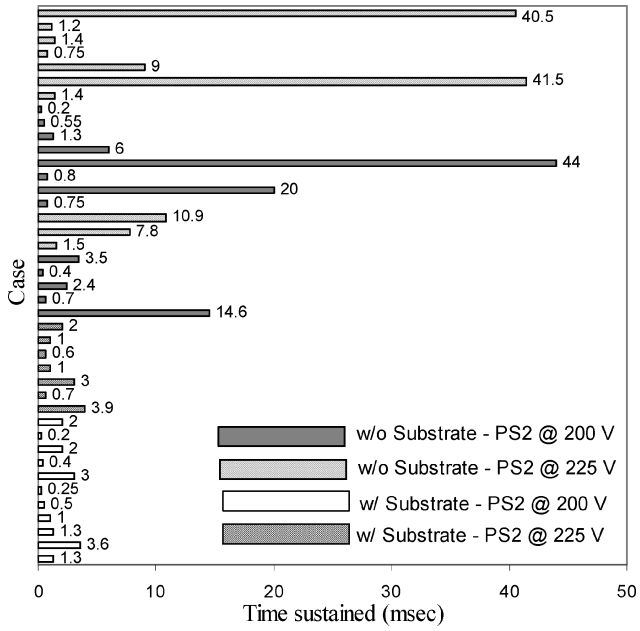

Fig. 18 Results of sustained-arc tests using the mock array coupon.

The possibility of controlling arc duration by choice of substrate materials would indeed be an attractive mitigation technique as it would be relatively easy to implement and could therefore reduce cost and risk for spacecraft manufacturers.

Conclusions

An experimental investigation has been conducted on solar-array samples to identify existing technologies that are most promising for direct-drive electric propulsion applications. The tests focused on the response of the arrays under operating conditions that promote arcing (negative bias). Hundreds of arc events were recorded during the tests. The results have been used to compare the capacity of two mainstream technologies to operate safely at high voltages, with significantly reduced or nonexistent chance for damage by sustained arcing. Voltage, current, and power limits have been identified. The test results yielded relatively low arcing thresholds for both technologies. If adjacent cells are not designed to operate below the sustained-arcing threshold, then arcs can lead to permanent damage of the array. Encapsulation can be used to eliminate arcs, but at a cost. Alternatively, it might be possible to decrease the likelihood of an arc occurring simply by changing the geometric layout of the cells in an existing solar array technology. Specifically, the cells could be arranged to minimize the occurrence of large voltage differences between cells in different strings. In addition, where large differential voltages do exist, the coverglass could be extended to cover the gap between strings. The additional coverglass will provide a physical barrier to the plasma particles. When plasma particles are stopped from entering the gap, arc initiation is eliminated. Although extending the coverglass has the same effect as encapsulation, with proper cell layout it is only necessary to extend the cover glass in specific areas and not over the entire array. The coverglass should be extended only over gaps between cells that have a high differential voltage and are therefore susceptible to sustained arcs.

Acknowledgments

This work was performed under NASA Glenn Research Center Contract NAS3-01100. The authors thank Ed Watts for his valuable assistance in gathering the arc data. We also acknowledge the contributions of the remaining D2HET team members, Andy Hoskins, Mary Hovater, David King, and M. Ralph Carruth.

References

[1]Oleson, S. R., and Myers, R. M., "Advanced Propulsion for Geostationary Orbit Insertion and North–South Station Keeping," *Journal of Spacecraft and Rockets*, Vol. 34, No. 1, 1997, pp. 22–28.

[2]Oleson, S. R., and Sankovic, J. M., "Advanced Hall Electric Propulsion for Future In-Space Transportation," NASA TM-2001-210676, April 2001.

[3]Hoskins, W. A., King, D., Kristalinksi, A., Kerslake, T., Peterson, T., Ferguson, D., Snyder, D., Jongeward, G., Mikellides, I., Carruth, R., Hovater, M., and Schneider, T., "Direct Drive Hall Thruster System Study," JANNAF Propulsion Meeting, Nov. 2002.

[4]Hamley, J. A., Sankovic, J. M., Miller, J. R., Lynn, P., O'neill, M. J., and Oleson, S. R., "Hall Thruster Direct Drive Demonstration," AIAA Paper 97-2787, July 1997.

[5]Vaughn, J. A., Carruth, M. R., Jr., Katz, I., Mandell, M. J., and Jongeward, G. A., "Electrical Breakdown Currents on Large Spacecraft in Low Earth Orbit," *Journal of Spacecraft and Rockets*, Vol. 31, No. 1, 1994, pp. 54–59.

[6]Mikellides, I. G., Jongeward, G. A., Schneider, T., Peterson, T., Kerslake, T. W., and Snyder, D., "Solar Arrays for Direct-Drive Electric Propulsion: Electron Collection at High Voltages," *Journal of Spacecraft and Rockets*, Vol. 42, No. 3, 2005, pp. 550–558.

[7]Davis, S., Stillwell, R., Andlario, W., Snyder, D., and Katz, I., "EOS-AM Solar Array Arc Mitigation Design," Society of Automotive Engineers, Paper 1999-01-2582, Aug. 1999.

[8]Ferguson, D. C., Snyder, D. B., Vayner, B. V., and Galofaro, J. T., "Array Arcing in Orbit–from LEO to GEO," AIAA Paper 99-0218, Jan. 1999.

[9]Hastings, D. E., Cho, M., and Kuninaka, H., "The Arcing Rate for a High Voltage Solar Array: Theory, Experiment and Predictions," *Journal Spacecraft and Rockets*, Vol. 29, No. 4, 1992, pp. 538–554.

[10]Ferguson, D. C., Hillard, G. B., Vayner, B. V., and Galofaro, J. T., "High Voltage Space Solar Arrays," International Astronautical Congress, Paper IAC-02-IAA.6.3.03, Oct. 2002.

[11]Cho, M., Ramasamy, R., Matsumoto, T., Toyoda, K., Nozake, Y., and Takahashi, M., "Laboratory Tests on 110-Volt Solar Arrays in Simulated Geosynchronous Orbit Environment," *Journal of Spacecraft and Rockets*, Vol. 40, No. 2, 2003, pp. 211–229.

[12]Vayner, B., Galofaro, J., Ferguson, D., and Degroot, W., "Electrostatic Discharge Inception on a High-Voltage Solar Array," AIAA Paper 2002-0631, Jan. 2002.

[13]Hikita, M., and Cho, M., "Charging and Discharging Phenomena in Simulated Space Environment," Inst. of Electrical and Electronics Engineers, 19th International Symposium on Discharges and Electrical Insulation in Vacuum, Paper 0-7803-5791-4/00, Sept. 2000.

[14]Cho, M., Shiraishi, K., Toyoda, K., and Hikita, M., "Laboratory Experiments on Mitigation Against Arcing on High Voltage Solar Array in Simulated LEO Plasma Environment," AIAA Paper 2002-0629, Jan. 2002.

[15]Jongeward, G. A., Mikellides, I. G., Peterson, T., Kerslake, T. W., Ferguson, D., Snyder, D., Carruth, M. R., Schneider, T., Hovater, M., Hoskins, A., King, D., and Ralph, E. L., "Development of a Direct Drive Hall Effect Thruster System," Society of Automotive Engineers, Paper 02PSC-77, Oct. 2002.

A. Ketsdever
Associate Editor